Search for Higgs boson pairs in the $b\bar{b}\gamma\gamma$ final state in ATLAS

Higgs Hunting 2023

Stockholm University, ATLAS Experiment.

Tom Ingebretsen Carlson

Introduction to $HH \rightarrow b\bar{b}\gamma\gamma$

Features of $HH \rightarrow b\bar{b}\gamma\gamma$:

- Gluon-gluon Fusion (**ggF**) and Vector Boson Fusion (**VBF**) production modes;

  $\sigma_{ggF} \sim 31.0$ fb and $\sigma_{VBF} \sim 1.73$ fb.

- **Very sensitive channel** – Despite its small BR (0.26%), it benefits from a clean $m_{\gamma\gamma}$ resolution ($\sigma_{\gamma\gamma}/M_{\gamma\gamma}$ =1.5%)

- Sensitive at low m_{hh} → **sensitive to κ_λ**

LO ggF diagrams:

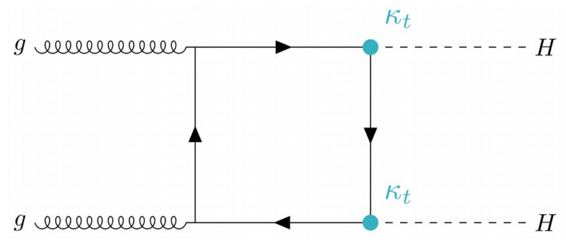

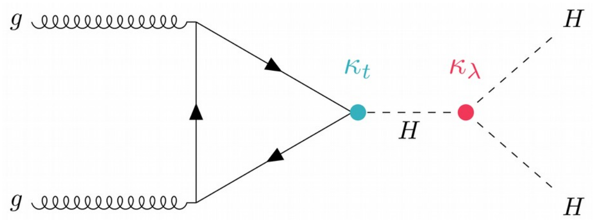

The κ-framework:

Higgs Trilinear coupling: λ_{HHH}

$$\kappa_\lambda = \lambda_{HHH}/\lambda^{SM}_{HHH}$$

$$\kappa_{2V} = g_{HHVV}/g^{SM}_{HHVV}$$

LO VBF diagrams:

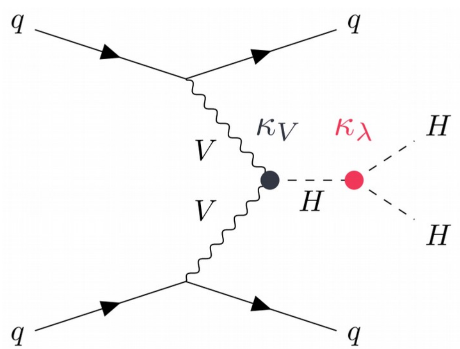

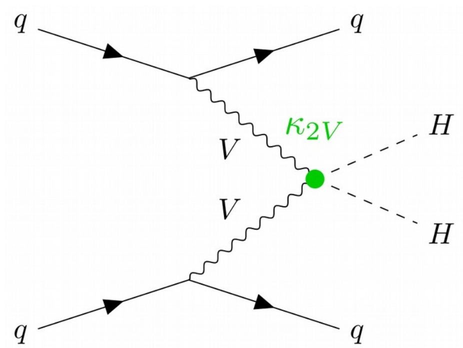

New non-resonant $b\bar{b}\gamma\gamma$ analysis, Ref: ATLAS-CONF-2023-050
Superseding and expanding upon the nonresonant results of Ref:**Phys. Rev. D 106 (2021) 052001**

Introduction to $HH \to b\bar{b}\gamma\gamma$

New non-resonant $b\bar{b}\gamma\gamma$ analysis: uses the same data set but supersedes and expands upon the previous nonresonant results.

Improvements of the new $HH \to b\bar{b}\gamma\gamma$ analysis:

- Optimization on both production modes
- Re-optimized BDT for classification of events
- Includes limits on κ_{2V}
- Effective Field Theory (EFT) interpretations

LO ggF diagrams:

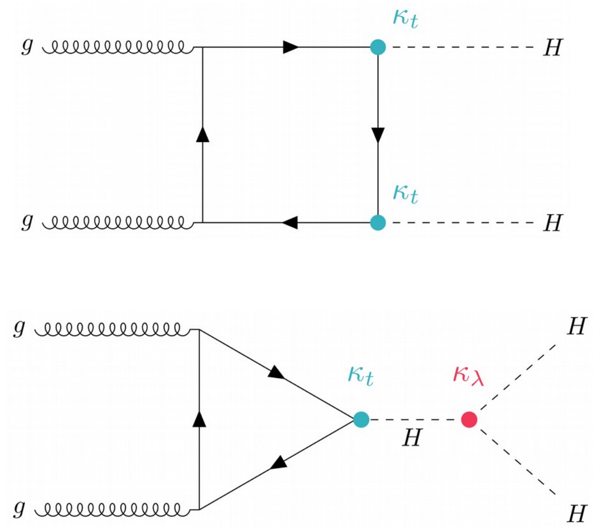

The κ-framework:

Higgs Trilinear coupling: λ_{HHH}

$$\kappa_\lambda = \lambda_{HHH} / \lambda^{\text{SM}}_{HHH}$$

$$\kappa_{2V} = g_{HHVV} / g^{\text{SM}}_{HHVV}$$

LO VBF diagrams:

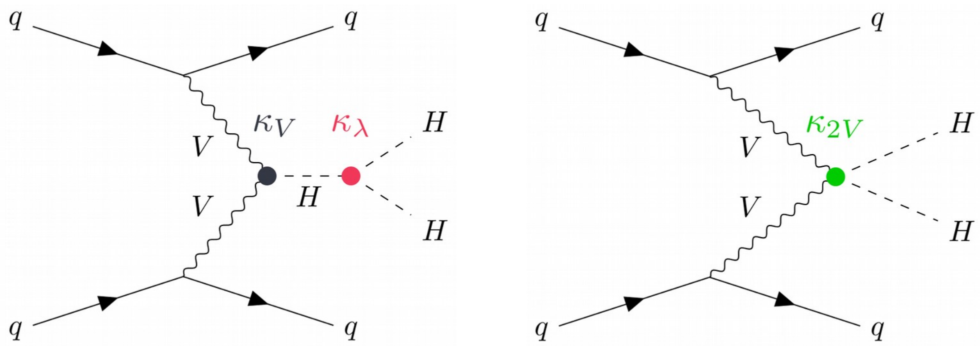

New non-resonant $b\bar{b}\gamma\gamma$ analysis, Ref: ATLAS-CONF-2023-050
Superseding and expanding upon the nonresonant results of Ref: Phys. Rev. D 106 (2021) 052001

Analysis strategy

Data
(2015-2018)
$\sqrt{s} = 13\,TeV,\ 140\,fb^{-1}$

Signal
ggF *HH*
VBF *HH*

Backgrounds
Non-resonant:
$\gamma\gamma$+jets
$t\bar{t}\gamma\gamma$
Resonant:
ggF H
VBF H
$t\bar{t}$H
(Full list in backup)

Preselection

Selected events:
- γγ trigger
- 2 photons with the WP of highest purity with $p_T/m_{\gamma\gamma} > 0.35$ (0.25)
- $105 < m_{\gamma\gamma} < 160$ GeV
- Exactly 2 b-jets at 77% efficiency

Rejected events:
- Events with leptons
- Events with > 5 central jets

Systematic uncertainties
Experimental
Modeling
(See backup for more)

Signal & Bkg models

Statistical Inference
- κ_λ and κ_{2V}
- Signal strength: μ
- **EFT interpretations**

Categorization
(Re-optimized BDT)

Signal strength: $\mu = \sigma/\sigma_{SM}$

Categorization and fitting strategy

Categorization of events:

High mass: $m^*_{b\bar{b}\gamma\gamma} > 350\mathrm{GeV}$ → targets small κ_λ values

Low mass: $m^*_{b\bar{b}\gamma\gamma} < 350\mathrm{GeV}$ → targets large κ_λ values

$$m^*_{b\bar{b}\gamma\gamma} = m_{b\bar{b}\gamma\gamma} - (m_{b\bar{b}} - 125) - (m_{\gamma\gamma} - 125)$$

Improves the signal mass resolution,
cancels detector resolution effects.

7 signal regions based on the BDT selection →

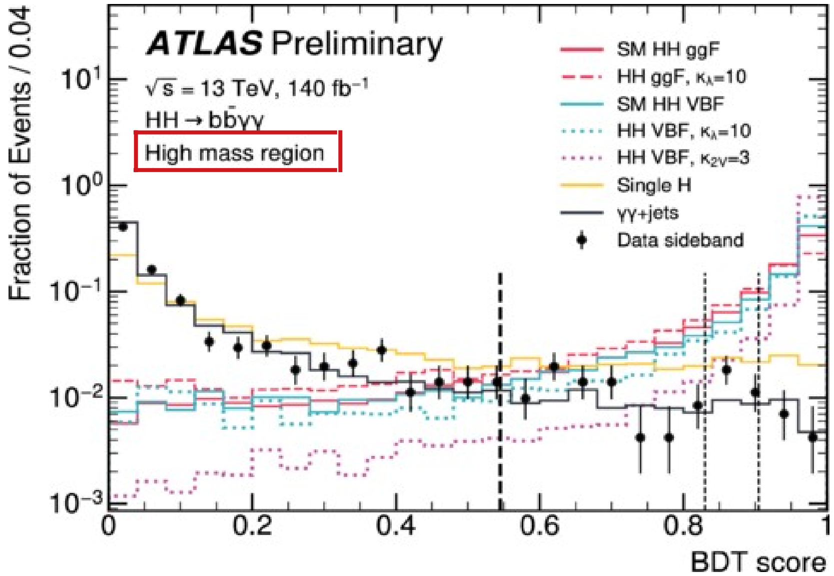

Signal and background modeling:

- Unbinned fits to $m_{\gamma\gamma}$
- HH signal & H background: Double-sided Crystal Ball function
- Nonresonant $\gamma\gamma$ bkg: Exponential function

New MC with improved statistics in the SRs.
→ **Reduced uncertainty on the signal yield (reduced uncertainty on the Spurious Signal[1])**

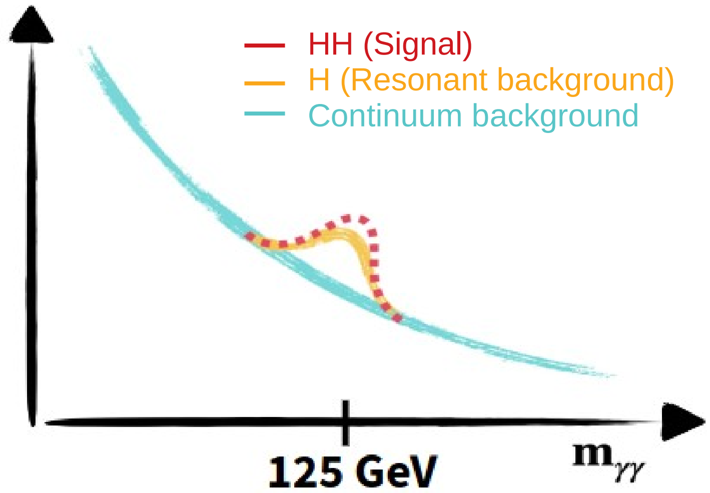

(BDT distributions for Low mass region in backup)

[1]Spurious signal is a non-zero signal obtained when fitting the signal plus background model to signal-free MC.

Results: signal strength, κ_λ and κ_{2V}

- No significant excess is observed in data (2015-2018)
- Results based on simultaneous unbinned maximum likelihood fit in all categories

Signal strength upper limits at 95% CL:

$\mu_{VBF+ggF}$ < 4.0 (< 5.0 expected, reduced by 12%)

Limits at 95% CL:

$-1.4 < \kappa_\lambda < 6.9$ ($-2.8 < \kappa_\lambda < 7.8$ expected, reduced by 6%)

$-0.5 < \kappa_{2V} < 2.7$ ($-1.1 < \kappa_{2V} < 3.3$ expected, reduced by 17%)

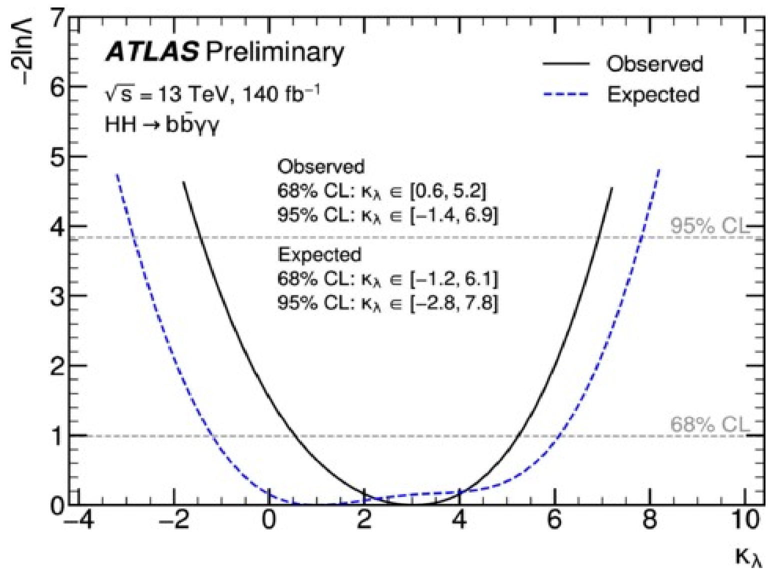

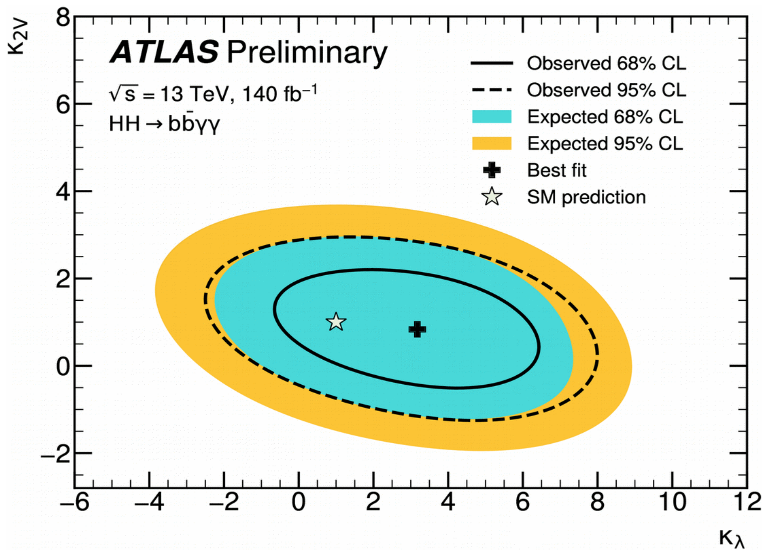

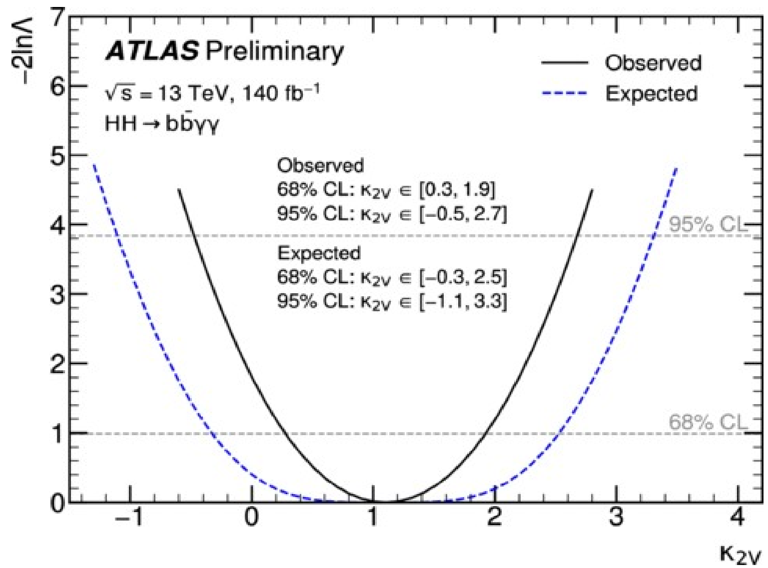

Effective Field Theory in $b\bar{b}\gamma\gamma$

EFTs: parameterize new Heavy physics in terms of higher dimensional operators and Wilson coefficients.

Two EFTs in $b\bar{b}\gamma\gamma$: SMEFT & HEFT

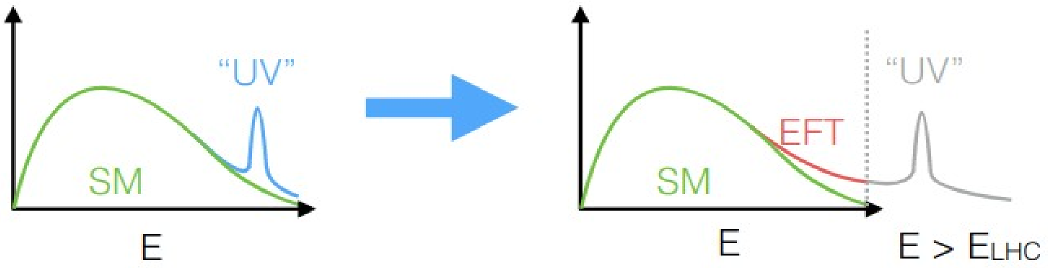

Standard Model Effective Field Theory (SMEFT):

- Extends the SM Lagrangian with higher dimensional operators

$$\mathcal{L}_{SMEFT} = \mathcal{L}_{SM} + \sum_{n} \sum_{i} \frac{c_i}{\Lambda^{2n}} \mathcal{O}_i^{4+2n}$$

- Higgs contained in SM doublet
- Dependencies in H background
- Interesting for global combinations
- Include relevant dimension-6 operators

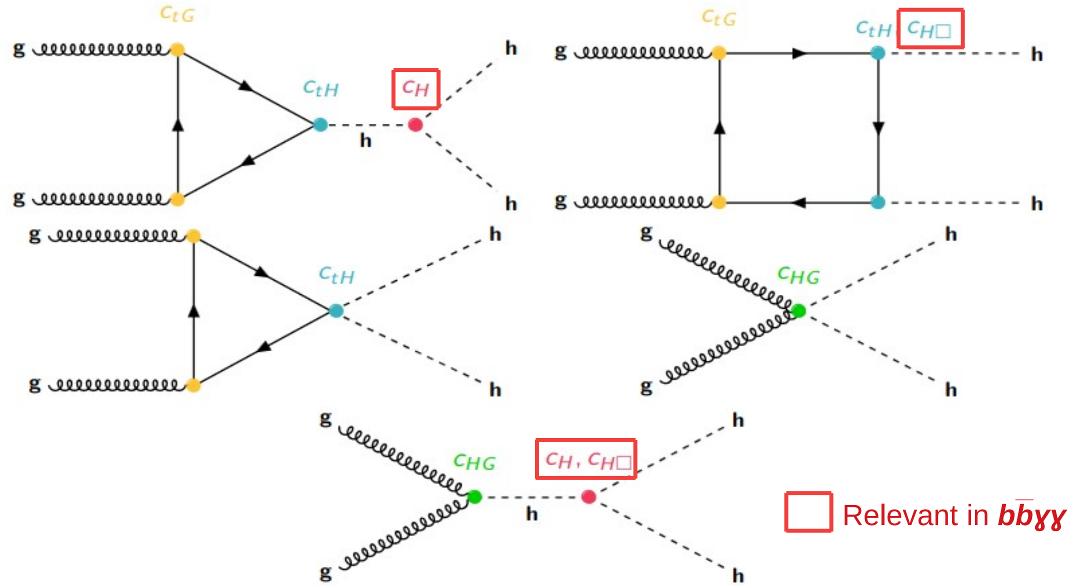

HH signal reweighting: as a function of truth m_{hh}

H background reweighting: as a function of truth H p_T

Example of generic LO ggF SMEFT diagrams.

Ref: Phys. Rev. D 103, 096024
JHEP 10 (2010) 085
arXiv:2304.01968

Effective Field Theory in $b\bar{b}\gamma\gamma$

EFTs: parameterize new Heavy physics in terms of higher dimensional operators and Wilson coefficients.

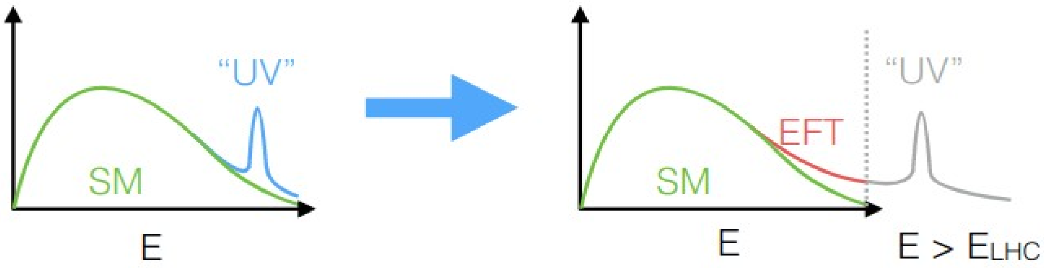

Two EFTs in $b\bar{b}\gamma\gamma$: SMEFT & HEFT

Higgs Effective Field Theory (HEFT) :

- Lagrangian built up by terms with increasing *chiral dimensions* χ or as successive loop order *L*:

$$\chi = 2L+2.$$

- Higgs is a singlet
- Can probe potential decorrelation among couplings
- More general than SMEFT
- Background is less dependent on HEFT than SMEFT

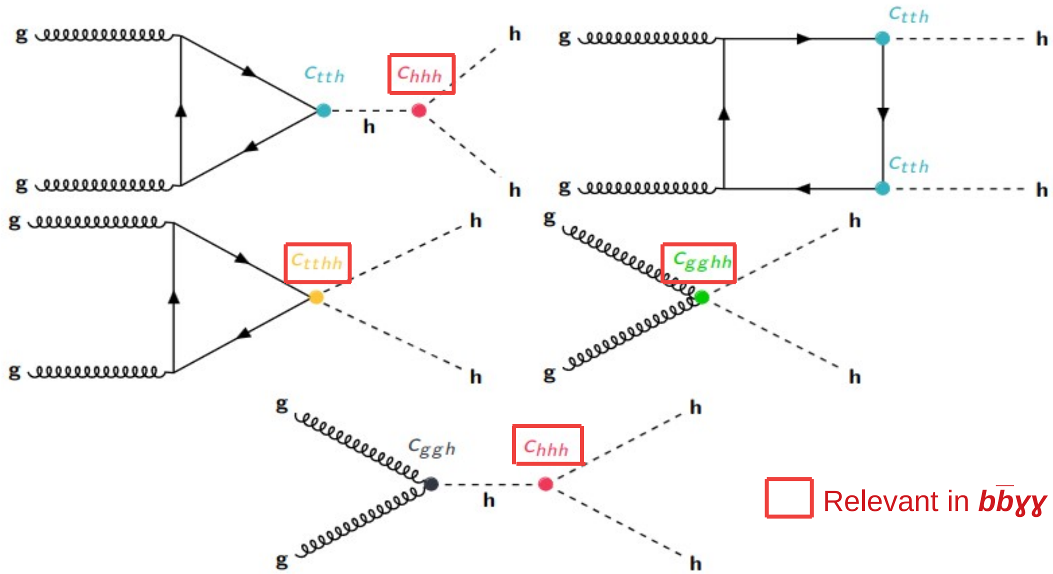

Example of generic LO ggF HEFT diagrams.

HH signal reweighting: as a function of truth m_{hh}

Ref: arXiv:2304.01968

Results: SMEFT

- Strongest SMEFT constraints in ATLAS from a single di-Higgs channel
- Results include linear and quadratic dependencies on the Wilson coefficients

Wilson coefficient	95% CL Observed	95% CL Expected
c_H	[−14.4, 6.2]	[−16.8, 9.7]
$c_{H\Box}$	[− 9.4, 10.2]	[−12.4, 13.7]

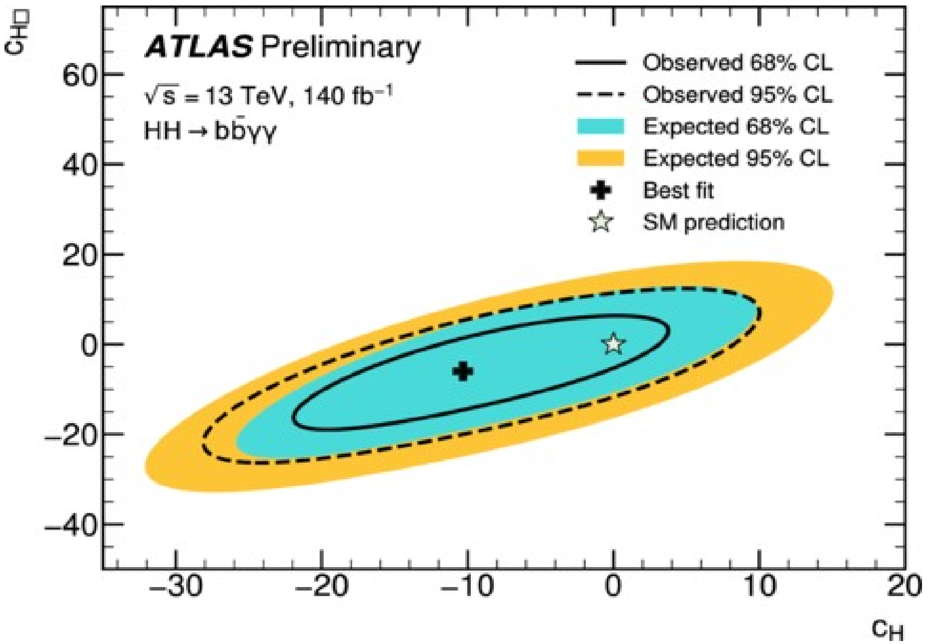

Results: HEFT

- Interpretations are made on HEFT m_{hh} shape benchmark points (BM)
- BM 3, 4, 5 and 7 are excluded at 95% CL

Wilson coefficient	95% CL Observed	95% CL Expected
c_{hhh}	[−1.8 , 7.7]	[−3.4 , 8.9]
c_{tthh}	[−0.42, 0.52]	[−0.59, 0.69]
c_{gghh}	[−0.28, 0.73]	[−0.48, 0.94]

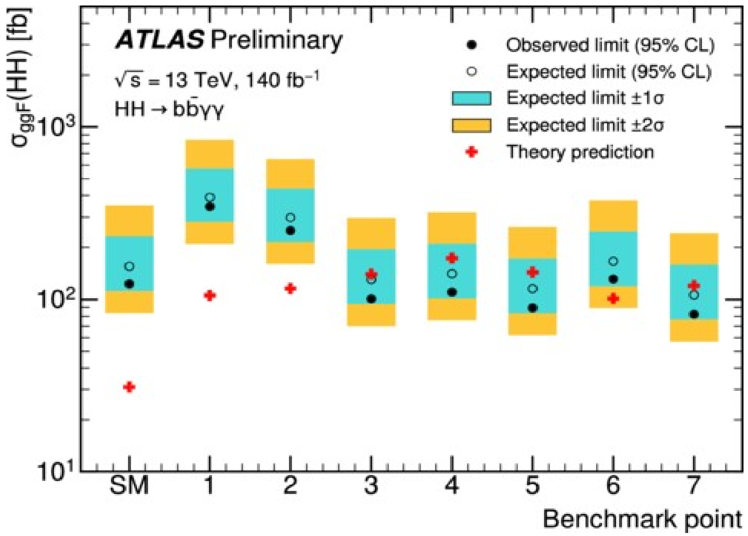

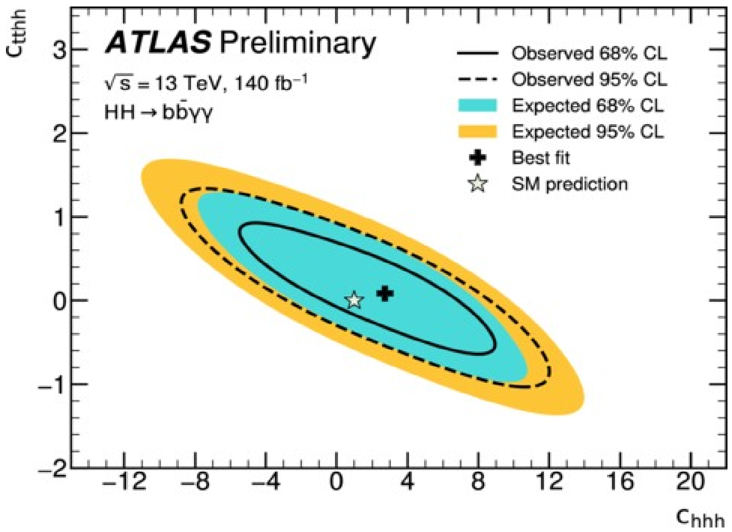

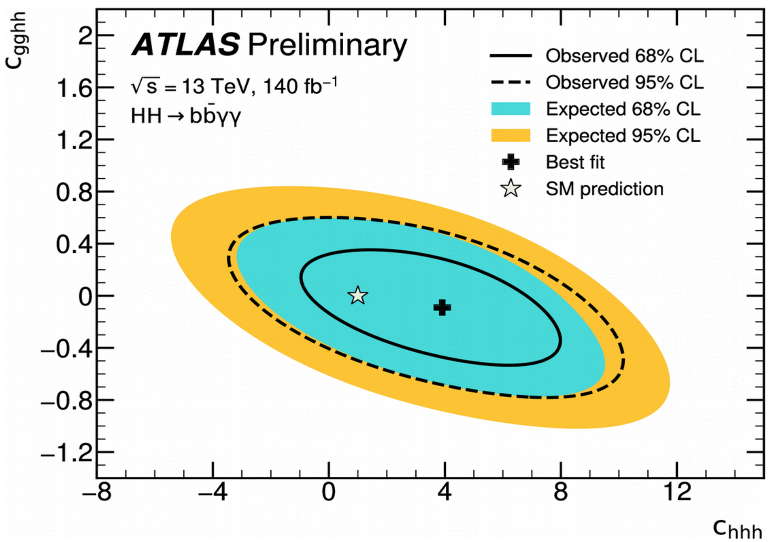

(Numerical values of HEFT BM points in backup)

Ref: JHEP 03 (2020) 091
arXiv:2304.01968

Thank you for your attention!

Backup

VBF: $m^*_{b\bar{b}\gamma\gamma}$ versus κ_λ

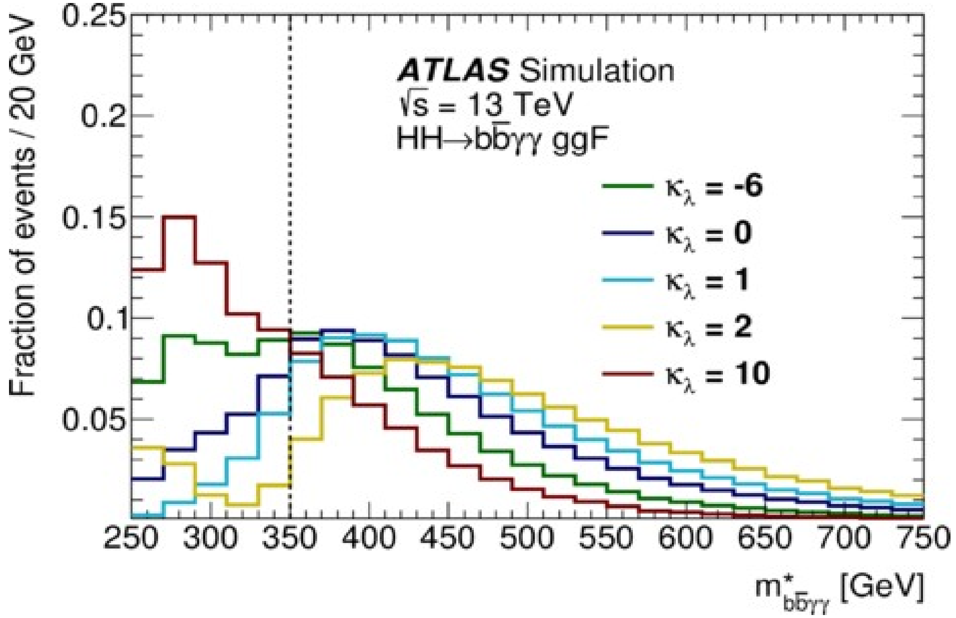

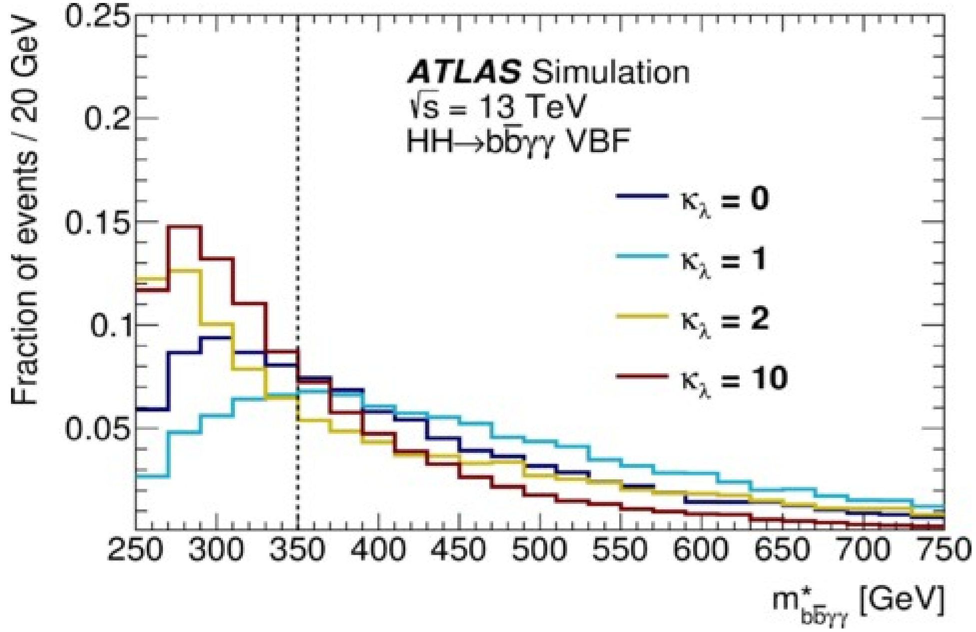

Monte Carlo samples

Process	Generator	PDF set	Showering	Tune
ggF HH	Powheg Box v2 [45–47]	PDF4LHC15NLO [48]	Pythia 8.2 [49]	A14 [50]
VBF HH	MadGraph5_aMC@NLO [51]	NNPDF3.0NLO [52]	Pythia 8.2	A14
ggF H	NNLOPS [53–57]	PDF4LHC15NLO	Pythia 8.2	AZNLO [58]
VBF H	Powheg Box v2 [45, 54, 59–65]	PDF4LHC15NLO	Pythia 8.2	AZNLO
WH	Powheg Box v2	PDF4LHC15NLO	Pythia 8.2	AZNLO
$qq \to ZH$	Powheg Box v2	PDF4LHC15NLO	Pythia 8.2	AZNLO
$gg \to ZH$	Powheg Box v2	PDF4LHC15NLO	Pythia 8.2	AZNLO
$t\bar{t}H$	Powheg Box v2 [60–62, 65, 66]	NNPDF3.0NLO	Pythia 8.2	A14
$b\bar{b}H$	Powheg Box v2	NNPDF3.0NLO	Pythia 8.2	A14
tHq	MadGraph5_aMC@NLO	NNPDF3.0NLO	Pythia 8.2	A14
tHW	MadGraph5_aMC@NLO	NNPDF3.0NLO	Pythia 8.2	A14
$\gamma\gamma$+jets	Sherpa 2.2.4 [67]	NNPDF3.0NNLO	Sherpa 2.2.4	–
$\gamma\gamma b\bar{b}$	Sherpa 2.2.12 [67]	NNPDF3.0NNLO	Sherpa 2.2.12	–
$t\bar{t}\gamma\gamma$	MadGraph5_aMC@NLO	NNPDF2.3LO	Pythia 8.2	A14

Systematic uncertainties

New non-resonant $b\bar{b}\gamma\gamma$ analysis:
Impact of uncertainties on the expected 95% CL upper limits on μ_{HH}.

Systematic uncertainty source	Relative impact [%]
Experimental	
Photon energy resolution	0.4
Photon energy scale	0.1
Flavor tagging	0.1
Theoretical	
Factorisation and renormalisation scale	4.8
$\mathcal{B}(H \to \gamma\gamma, b\bar{b})$	0.2
Parton showering model	0.2
Heavy-flavor content	0.1
Background model (spurious signal)	0.1

Previous $b\bar{b}\gamma\gamma$ analysis

		Relative impact of the systematic uncertainties [%]	
Source	Type	Nonresonant analysis HH	Resonant analysis $m_X = 300$ GeV
Experimental			
Photon energy resolution	Norm. + Shape	0.4	0.6
Jet energy scale and resolution	Normalization	< 0.2	0.3
Flavor tagging	Normalization	< 0.2	0.2
Theoretical			
Factorization and renormalization scale	Normalization	0.3	< 0.2
Parton showering model	Norm. + Shape	0.6	2.6
Heavy-flavor content	Normalization	0.3	< 0.2
$\mathcal{B}(H \to \gamma\gamma, b\bar{b})$	Normalization	0.2	< 0.2
Spurious signal	Normalization	3.0	3.3

BDT & categorization

Additional info

- One BDT in HM and one in LM
- Trained to distinguish between signal and H→γγ, $t\bar{t}\gamma\gamma$ and γγ+jets
- XGboost is used.
- Signal samples: SM ggF HH, SM VBF HH and κ_λ = {1, 10, 5.6}.

The category division: decided by maximizing the combined number-counting significance

Input variables:

- Baseline variables (same as previous analysis, see table) + additional variables and VBF-jet tagger.
- VBF-jet tagger: classifying events with 4 or more jets. Feeding as input jet kinematics.
- Additional variables: m^*_{bbyy}, ΔR and event shape variables transverse sphercity, planar flow and momentum balance.

Variable	Definition
Photon-related kinematic variables	
$p_T/m_{\gamma\gamma}$	Transverse momentum of each of the two photons divided by the diphoton invariant mass $m_{\gamma\gamma}$
η and ϕ	Pseudorapidity and azimuthal angle of the leading and subleading photon
Jet-related kinematic variables	
b-tag status	Tightest fixed b-tag working point (60%, 70%, or 77%) that the jet passes
p_T, η and ϕ	Transverse momentum, pseudorapidity and azimuthal angle of the two jets with the highest b-tagging score
$p_T^{b\bar{b}}$, $\eta_{b\bar{b}}$ and $\phi_{b\bar{b}}$	Transverse momentum, pseudorapidity and azimuthal angle of the b-tagged jets system
$m_{b\bar{b}}$	Invariant mass of the two jets with the highest b-tagging score
H_T	Scalar sum of the p_T of the jets in the event
Single topness	For the definition, see Eq. (1)
Missing transverse momentum variables	
E_T^{miss} and ϕ^{miss}	Missing transverse momentum and its azimuthal angle

BDT score distribution

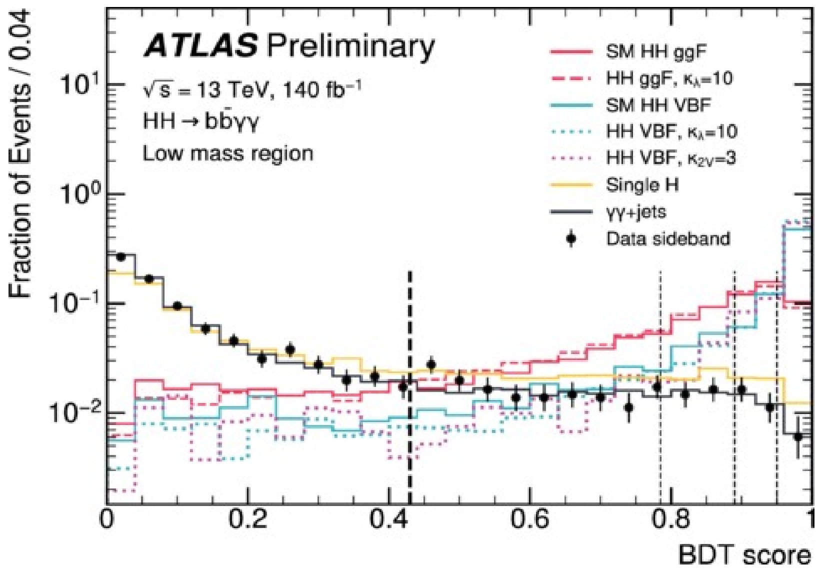

*M*γγ distributions: Data vs. bkg fit

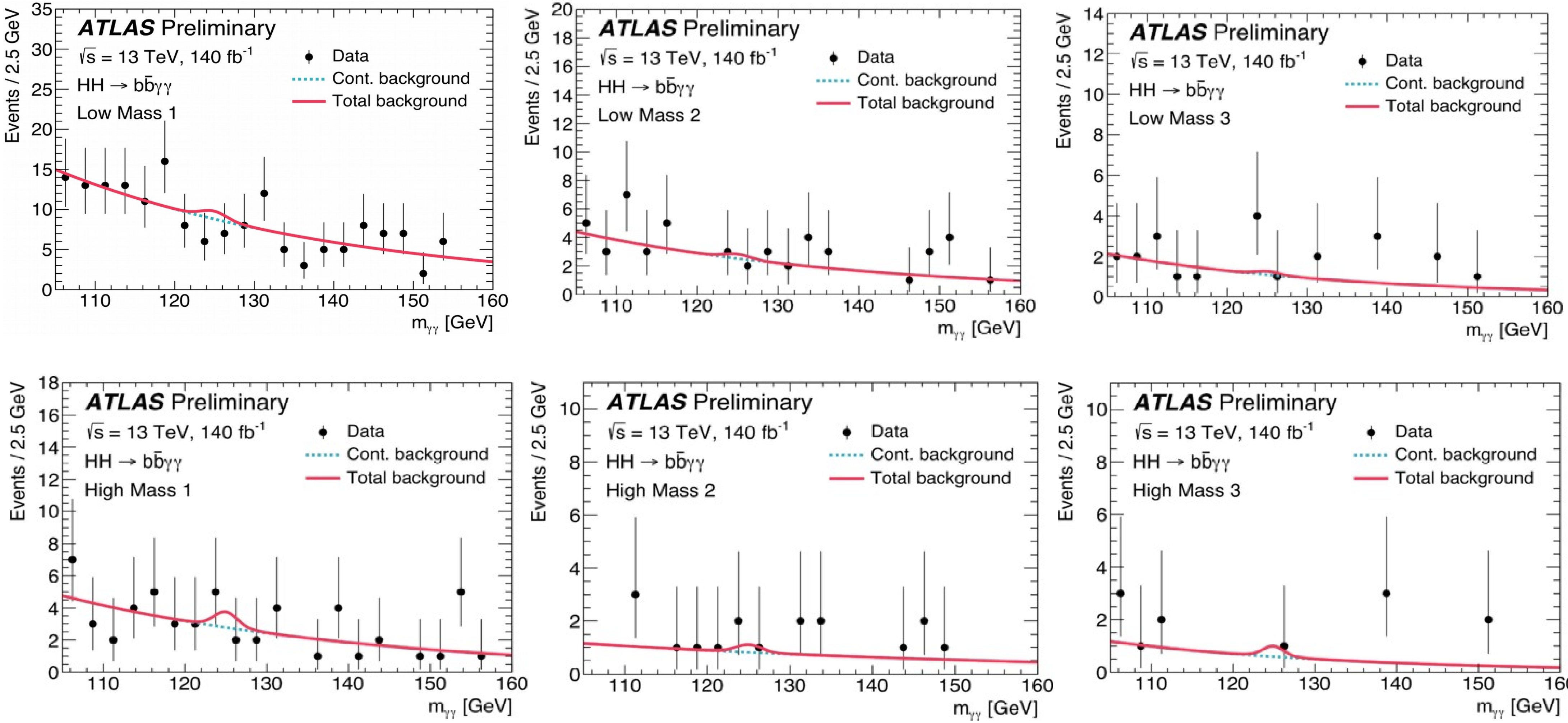

Results: signal strength, κ_λ and κ_{2V}

This $b\bar{b}\gamma\gamma$ analysis:
Limits at 95% CL:

$-1.4 < \kappa_\lambda < 6.9$ ($-2.8 < \kappa_\lambda < 7.8$ expected)

$-0.5 < \kappa_{2V} < 2.7$ ($-1.1 < \kappa_{2V} < 3.3$ expected)

Previous $b\bar{b}\gamma\gamma$ analysis:
Limits at 95% CL:

$-1.4 < \kappa_\lambda < 6.5$ ($-3.2 < \kappa_\lambda < 8.1$ expected)

$-0.8 < \kappa_{2V} < 3.0$ ($-1.6 < \kappa_{2V} < 3.7$ expected)

Improvements compared to previous analysis:
Expected limits:

- $\mu_{VBF+ggF}$ - reduced by 12%.
- Width of 1D confidence interval κ_λ (κ_{2V}) – reduced by 6% (17%).

Observed limits:

- μ_{HH} - reduced by 5%.
- Width of 1D confidence interval κ_λ (κ_{2V}) – increased by 5% (reduced by 16%).

Additional signal strength limits:

$\mu_{ggF} < 4.1$ (< 5.3 expected)

$\mu_{VBF} < 96$ (< 145 expected)

EFT Lagrangian's

$$\Delta\mathcal{L}_{\text{Warsaw}} = \frac{C_{H,\Box}}{\Lambda^2}(\phi^\dagger\phi)\Box(\phi^\dagger\phi) + \frac{C_{HD}}{\Lambda^2}(\phi^\dagger D_\mu\phi)^*(\phi^\dagger D^\mu\phi) + \frac{C_H}{\Lambda^2}(\phi^\dagger\phi)^3$$
$$+ \left(\frac{C_{uH}}{\Lambda^2}\phi^\dagger\phi\bar{q}_L\tilde{\phi}\,t_R + h.c.\right) + \frac{C_{HG}}{\Lambda^2}\phi^\dagger\phi G^a_{\mu\nu}G^{\mu\nu,a}$$
$$+ \frac{C_{uG}}{\Lambda^2}(\bar{q}_L\sigma^{\mu\nu}T^a G^a_{\mu\nu}\tilde{\phi}\,t_R + \text{h.c.})\,.$$

$$\Delta\mathcal{L}_{\text{HEFT}} = -m_t\left(c_t\frac{h}{v} + c_{tt}\frac{h^2}{v^2}\right)\bar{t}\,t - c_{hhh}\frac{m_h^2}{2v}h^3$$
$$+ \frac{\alpha_s}{8\pi}\left(c_{ggh}\frac{h}{v} + c_{gghh}\frac{h^2}{v^2}\right)G^a_{\mu\nu}G^{a,\mu\nu}\,.$$

Additional EFT information

HEFT shape BM points
represent different m_{hh} shapes

Benchmark	c_{hhh}	c_{tth}	c_{ggh}	c_{gghh}	c_{tthh}
SM	1	1	0	0	0
1	5.11	1.10	0	0	0
2	6.84	1.03	-1/3	0	1/6
3	2.21	1.05	1/2	1/2	-1/3
4	2.79	0.90	-1/3	-1/2	-1/6
5	3.95	1.17	1/6	-1/2	-1/3
6	-0.68	0.90	1/2	0.25	-1/6
7	-0.10	0.94	1/6	-1/6	1

Signal reweighting
SMEFT and HEFT signal is parametrized as a function of m_{hh}

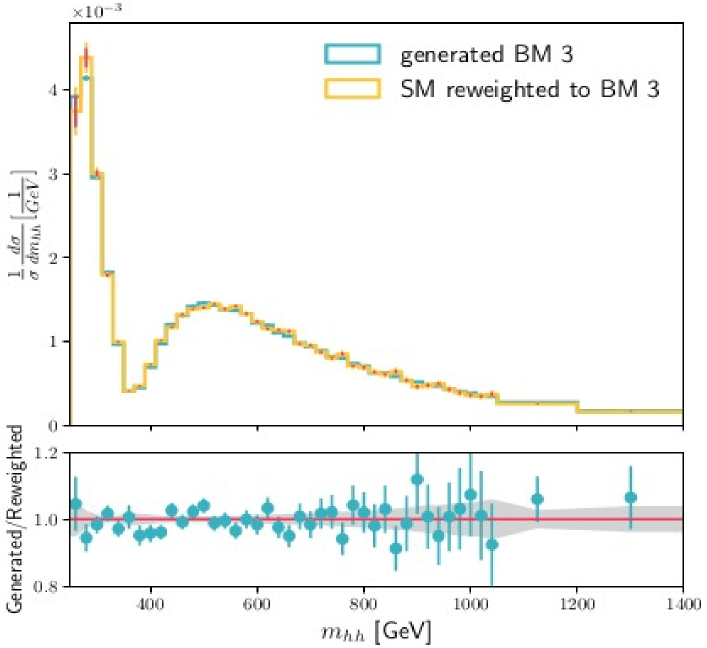

Ref: arXiv:2304.01968

SMEFT truncation scheme

$$|\mathcal{M}_{\mathrm{SMEFT}}|^2 = |\mathcal{M}_{\mathrm{SM}}|^2 + \underbrace{\sum_i \frac{c_i^{(6)}}{\Lambda^2} 2\mathrm{Re}\left(\mathcal{M}_i^{(6)} \mathcal{M}_{\mathrm{SM}}^*\right)}_{\text{linear model}} + \underbrace{\sum_i \frac{\left(c_i^{(6)}\right)^2}{\Lambda^4} \left|\mathcal{M}_i^{(6)}\right|^2}_{\text{quadratic terms}} + \underbrace{\sum_{i<j} \frac{c_i^{(6)} c_j^{(6)}}{\Lambda^4} 2\mathrm{Re}\left(\mathcal{M}_i^{(6)} \mathcal{M}_j^{(6)*}\right)}_{\text{cross terms}} + \ldots$$

$HH \to b\bar{b}b\bar{b}$: EFT limits

Parameter	Expected Constraint		Observed Constraint	
	Lower	Upper	Lower	Upper
c_H	−20	11	−22	11
c_{HG}	−0.056	0.049	−0.067	0.060
$c_{H\Box}$	−9.3	13.9	−8.9	14.5
c_{tH}	−10.0	6.4	−10.7	6.2
c_{tG}	−0.97	0.94	−1.12	1.15

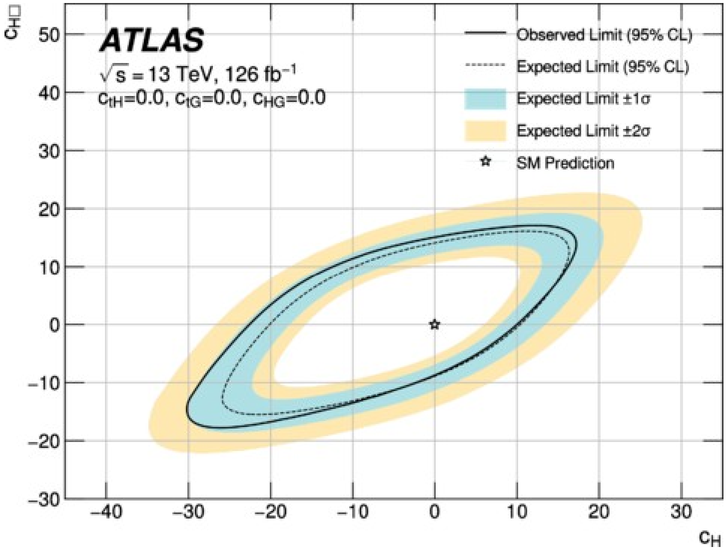

HEFT observed (expected limits):

c_{ggHH} : $[-0.36, 0.78]([-0.42, 0.75])$

c_{ttHH} : $[-0.55, 0.51]([-0.46, 0.40])$

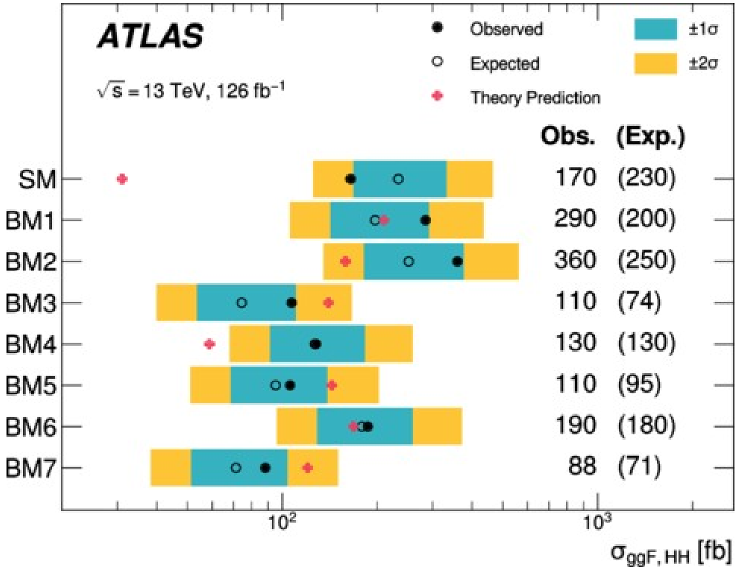

Sensitivity of di-Higgs channels

Upper limits on *HH* signal strength at 95% CL for the different *HH* channels. Ref: Phys. Lett. B 843 (2023) 137745

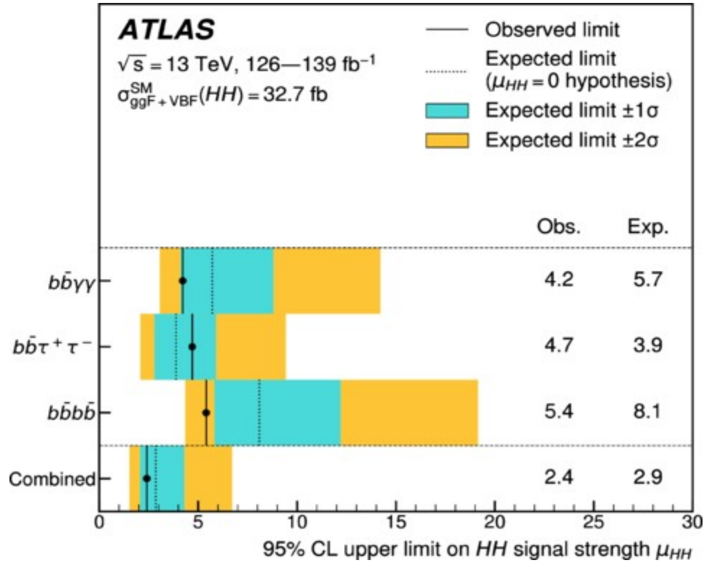

Cross section limits on a BSM scalar X from the different HH channels. Ref: ATLAS-CONF-2021-052